

# Normative Blood Flow Values in the Posterior Fossa using Quantitative Spin-Echo DSC Perfusion MRI

J. J. Mouannes<sup>1</sup>, A. Aghaei-Lasboo<sup>2</sup>, A. H. Yassari<sup>3</sup>, A. Sen<sup>2</sup>, A. Skolnik<sup>3</sup>, S. Rahimi<sup>2</sup>, T. J. Carroll<sup>1,2</sup>, B. R. Bendok<sup>4</sup>, M. T. Walker<sup>2</sup>, S. W. Horowitz<sup>2</sup>, and A. Shaibani<sup>2</sup>

<sup>1</sup>Biomedical Engineering, Northwestern University, Chicago, IL, United States, <sup>2</sup>Radiology, Northwestern University, Chicago, IL, United States, <sup>3</sup>Feinberg School of Medicine, Northwestern University, Chicago, IL, United States, <sup>4</sup>Neurological Surgery, Northwestern University, Chicago, IL, United States

## INTRODUCTION

Stroke is the second leading cause of death and disability. The interest in cerebral perfusion imaging has increased in recent years, with the aim of accurately detecting and categorizing brain tissue at risk of infarction, also known as the “ischemic penumbra” [1-3]. These efforts have resulted in the establishment of normal perfusion parameters such as cerebral blood flow (CBF), cerebral blood volume (CBV), and mean transit time (MTT), for the supratentorial section of the brain in order to calculate ischemic thresholds and identify salvageable brain tissue [4,5]. However, without a quantitative understanding of the normal flow values for the posterior fossa structures, it is difficult to make judgments on issues such as cerebrovascular reserve or chronic ischemia. This is particularly true for the posterior fossa structures which derive their flow primarily from a single artery (the basilar artery), which precludes side-to-side comparison such as is done for the supratentorial brain [6-8]. Therefore, we have performed an evaluation of normative “quantitative” perfusion values for the posterior fossa in adults using the Bookend technique [9,10], which has been proven reliable and reproducible [11].

## MATERIALS AND METHODS

38 patients (23 females and 15 males) were retrospectively studied after being scanned on a 1.5 T MR scanner (Avanto, Siemens Medical Solutions, Erlangen, Germany) using the Bookend technique. 8 healthy normal volunteers (3 females and 5 males) were scanned with the same protocol on a 1.5 T MR scanner (MAGNETOM Espree, Siemens AG Healthcare Sector, Erlangen, Germany). T<sub>2</sub>-weighted spin-echo (SE) dynamic susceptibility contrast (DSC) images were obtained during the second bolus injection of a single dose of gadolinium-based contrast agent at a rate of 4 ml/s. Typical SE echo planar imaging (EPI) parameters were: TE/TR = 72/1500 ms, FOV/matrix = 220 mm x 200 mm/128 x 128, flip angle = 90°, 2-fold parallel imaging acceleration (GRAPPA). The Bookend technique quantifies cerebral perfusion based on T<sub>1</sub> changes in white matter and the blood pool, resulting from the contrast injection [10], using Look-Locker EPI with the following parameters: TE/TR = 9.9/21 ms, flip angle = 20°, FOV/matrix = 220 mm x 220 mm/128 x 128. The selection of patients was based on pathology or indications that would not result in abnormal posterior fossa perfusion. The different posterior fossa areas studied were: the midbrain, the vermis, the superior cerebellar artery (SCA) territory, the pons, the middle cerebellar peduncles (MCP), the posterior inferior cerebellar artery (PICA) territory, and the medulla. An ROI analysis of supratentorial white matter (WM) and gray matter (GM) perfusion and perfusion values recorded in the healthy volunteers served as internal and external controls, respectively.

## RESULTS

The results for quantitative CBF (qCBF), quantitative CBV (qCBV) and MTT showed relative consistency when comparing patients vs. volunteers for the posterior fossa structures as well as supratentorial WM and GM. Table 1 compares quantitative perfusion values in patients and healthy volunteers (controls) for the posterior fossa and supratentorial tissues (p>0.05 for most of the regions). Figure 1 displays qCBF images of 9 contiguous slices covering the sub- and supratentorial regions.

**Table 1.** qCBF, qCBV, and MTT in sub- and supratentorial regions for patients and healthy controls.

	qCBF (ml/(100g-min))			qCBV (ml/100g)			MTT (sec)		
Brain Region	Patients	Controls	p-value	Patients	Controls	p-value	Patients	Controls	p-value
Midbrain	35.9±7	43.5 ± 13	0.15	2.7±0.6	2.6 ± 0.6	0.68	4.7±0.9	4.0 ± 1.1	0.14
Vermis	35.9±8	49.6 ± 9.8	0.01	2.6±0.6	3.0 ± 0.9	0.27	4.7±0.75	3.9 ± 0.6	0.01
SCA Territory	42.5±9.5	50.3 ± 12	0.13	3.0±0.7	3.1 ± 0.7	0.72	4.6±0.7	3.8 ± 0.8	0.03
Pons	48.9±10	54.9 ± 15	0.32	3.8±0.7	3.3 ± 0.8	0.14	5.2±0.8	3.9 ± 0.9	0.01
MCP	29.7±5	24.1 ± 9	0.13	2.1±0.4	1.2 ± 0.6	0.005	4.6±0.9	3.5 ± 1.4	0.07
PICA Territory	62.1±13	50.2 ± 11	0.03	4.6±1	3.0 ± 0.7	0.001	6.6±1	4.1 ± 0.7	0.00
Medulla	28.9±5	33.1 ± 13	0.40	2.2±0.5	1.8 ± 0.7	0.17	5.1±0.95	4.0 ± 1.3	0.06
Supratentorial WM	19.9±5	24.7 ± 6	0.07	1.5±0.4	1.7 ± 0.3	0.15	4.8±1.2	4.6 ± 1.0	0.64
Supratentorial GM	51.1±8	60.5 ± 12	0.07	3.6±0.65	3.5 ± 0.7	0.72	4.3±0.5	3.7 ± 0.5	0.02

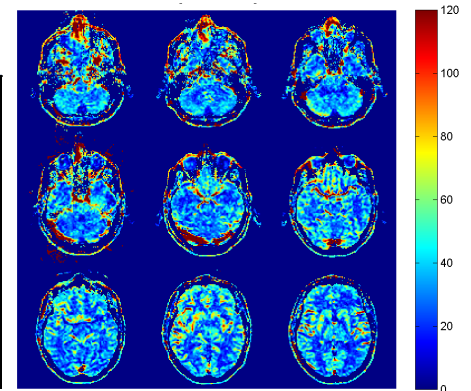


**Figure 1.** Parametric images of qCBF (ml/(100g-min)) for 9 contiguous slices.

## DISCUSSION/CONCLUSIONS

We have quantified cerebral perfusion in the posterior fossa for the first time using DSC MRI, with a Bookend technique implementation. SE DSC was performed for producing T<sub>2</sub>-weighted images of subtentorial brain where field inhomogeneity results in signal dropout in T<sub>2</sub>\*-weighted gradient-echo DSC images [12]. Supratentorial (WM and GM) qCBF and qCBV values in patients were also in accordance with the ones measured in normal volunteers, proving the reliability of the technique. We have, therefore, established a trustworthy reference for the posterior fossa blood flow in the human brain, which could be helpful in assessing patients with neurodegenerative diseases of the posterior fossa.

## REFERENCES

- [1] Pomerantz et al. Seminars in Ultrasound, CT, and MRI. 27:243-70 (2006).
- [2] Ueda et al. AJNR 20:983-9 (1999).
- [3] Wittsack et al. Radiology 222:397-403 (2002).
- [4] Baron et al. Cerebrovascular Disease 11 Suppl 1:2-8 (2001).
- [5] Bristow et al. J Cereb Blood Flow Metab 25:1280-7 (2005).
- [6] Lee et al. Radiology 153:137-43 (1984).
- [7] Mirzai et al. Keio J Med 49 Suppl 1:A45-50 (2000).
- [8] Randell et al. Am J Roentgenol 141:489-96 (1983).
- [9] Salaie et al. JMRI 21:512-519 (2005).
- [10] Shin et al. MRM 56:138-145 (2006).
- [11] Shin et al. MRM 58(6):1232-41 (2007).
- [12] Carroll et al. MRI (2008) – in press.